Faraday cup design for low power electric thrusters

SPACE PROPULSION 2020+1

17 - 18 - 19 MARCH 2021

V.Hugonnaud[1,2], **S.Mazouffre**[2], **D.Krejci**[1], **C.Scharlemann**[3], and **B.Seifert**[4]

[1]*Enpulsion, Viktor kaplan straße 2700, Wienner Neustadt, Austria*
[2]*CNRS-ICARE, 3 Avenue de la Recherche Scientifique, 45100 Orléans, France*
[3]*University of Applied Sciences Fachhochschule, Johannes Gutenberg-Straße 3, Wiener Neustadt, 2700, Austria*
[4]*FOTEC Forschungs- und Technologietransfer GmbH, Wiener Neustadt, 2700, Austria*

January 22, 2021

Keywords

Faraday cup, plasma diagnostic, low power electric thruster, ion collection efficiency

Abstract

This paper deals with plasma diagnostic in the frame of the plume study of low power electric propulsion (EP) devices. The work introduces information enabling optimization and standardization of an electrostatic plasma diagnostic known as Faraday Cup (FC). This instrument is used to accurately map in two or three dimensions the ion beam profile produced by an electric propulsion (EP) device [1, 2, 3, 4]. Results focus on the design of a Faraday cup in terms of probe aperture diameter, collection solid angle and material exposed to the ion beam. Additionally, modification of the equipotential field lines inside the probe are studied. The goal is to contribute to the effort towards repetitive and reliable determination of an EP device performance map (i.e. thrust, divergence angle, ionization efficiency and propellant utilization).

1 Introduction

The demand for low-power electric propulsion devices ($< 200\,W$) enabling precise, cost-effective orbital manoeuvres (orbit and attitude control, orbit transfer) for small satellites has increased for the last years [5, 6, 7]. Hence, many thruster manufacturers provide their own solution/technology (Hall Thrusters, Gridded Ion Engines, FEEPs) to satellite manufacturers and operators to fulfil their needs [8, 9, 10, 11]. As each technology relies on different parameters (propellant, ion energy, current density, ionisation, and acceleration processes) it is currently difficult to assess plume properties and provide accurate performance comparison in terms of thrust level, propellant utilization, beam energy and divergence angle. One technique to determine the ion flow properties of an electric thruster, therefore accessing performance information is to use electrostatic probes [1]. It basically consists of a conducting electrode, termed the collector, polarized to a high negative voltage with respect to the local floating potential to repel electrons and capture ions. There are various configurations of probes from a simple metal disk to architectures with collimator, filters and guard rings. The following paper deals with the investigation of the ion flow properties produced by two types of electric thrusters, namely Field-Emission-Electric-Propulsion (FEEP) devices and Hall Thrusters (HT) with a specific type of electrostatic probe, Faraday cups (FC). In this work, the FEEP thruster is the 40 W-class *ENPULSION NANO* laboratory unit from ENPULSION [12, 13, 14] and the Hall thruster is the 200 W-class ISCT200 from the CNRS-ICARE laboratory [15, 16]. Together, these two technologies cover a wide range of ion energy (0.2 keV – 10 keV) and ion current density (from $\mu A/cm^2$ to mA/cm^2) for different ions species such as indium (FEEP) and xenon (HT). Faraday cups measurements are sensitive to these parameters since they play a role in charge exchange collisions (CEX), ion induced electron emission (IIEE), sputtering and material deposition. Those phenomena have a direct impact on the Faraday cup output. The same Faraday cup design was used while different parameters (material, geometry, applied potential) were tested. First, different electric field inside the cup were used. Combination of different potentials applied to the cup and to the collimator were studied to maximize ion collection and minimize IIEE due to highly energetic ion impact on the cup. To the same end, different materials (molybdenum, graphite and aluminium) for the collimator were studied. Finally, different collimator/cup aspect ratios were chosen to study the impact of the FC diameter on signal output. Combining all results allows optimization of the FC design for high precision measurements and definition of a universal FC architecture able to cover of broad range of plasma plume characteristics.

2 Experimental apparatus

2.1 Vacuum chambers, mechanical interface and instrument

The FEEP thruster *ENPULSION NANO* plume was studied at ENPULSION at the FH Wiener Neustadt's electric propulsion laboratory in Austria. Measurement in the Hall thruster ISCT200 plume was performed at the ICARE EP laboratory in France.
Experiments with the HT were performed in the cryogenically pumped NExET (New Experiments on Electric Thrusters) vacuum chamber. NExET is based on a 1.8 m in length and 0.8 m in diameter stainless steel tank [17]. The overall pump stack warrants a background pressure as low as 2×10^{-5} mbar-Xe during operation of a 200 W input power plasma source. In the case of the FEEP thruster, the latter was studied while firing inside a cylindrical stainless-steel vacuum tank of 0.67 m in diameter and 1.32 m in length. The residual pressure in the tank goes down to 10^{-7} $mbar$. During operation of the FEEP thruster the pressure level is typically 4×10^{-6} $mbar$. The grounded vacuum chambers are used as potential reference for each thruster experiment series.
Both test campaign use similar set-up. The Faraday cup is attached to an aluminium structure designed to automatically align the probe with the thruster equatorial plane. The mechanical frame is mounted on a URS1000BCC motorized rotation stage and controlled by a SMC100 unit provided by Newport. The pivot point of the rotating structure is aligned with both the thruster axis and exit plane. The system enable a 180° scan on the horizontal plane with respect to the thruster. Its centreline is referred to as the 0° angular position of the probe. An in-house program is used to synchronize all devices to enable accurate control, to record and to save measured data. Note that all current density profiles scan the ion beam from -90° to 90° with step size of 2° and 1° for the FEEP and HT respectively .
The distance between the FC entrance and the thruster exit plane (R) is here limited by the vacuum chamber diameter. Consequently, For the ISCT200 R is fixed at 27.4±0.2 cm ($\sim$6 thruster mean channel diameters). For the *ENPULSION NANO* laboratory unit R is 26.1 cm. There, R is in excess of 15 emitter crown diameters. The far field plume is usually defined as the region where R is greater than four thruster diameters [18]. In the far-field plume domain the thruster is assumed to be a point ion source [19, 20, 3]. Therefore, the point source hypothesis is valid for both thruster studies. In both cases the entire mechanical structured is refereed to the experiment ground.
Calibrated Keithley 2410 and 2050 sourcemeters in voltage source mode have been used to measure the ion current collected by the Faraday cup collector and the collimator electrode. All instruments are referenced to the experiment common ground.

2.2 Laboratory unit thrusters: The ISCT200 and *ENPULSION NANO*

Hall thrusters are electrical propulsion devices that use a plasma discharge with magnetized electrons to ionize and accelerate a propellant gas [3, 21, 8, 22]. The principle relies upon a magnetic barrier and a low-pressure dc discharge generated between an external cathode and an anode, see figure 1 (top). The latter is located at the upstream end of a coaxial annular dielectric channel that confines the discharge. A fraction of the electrons emitted by the thermionic cathode flows downstream to neutralize the ion beam. The remaining part travels toward the anode to maintain the plasma discharge. The propellant gas, typically xenon, is introduced at the back of the channel. Magnetizing coils or permanent magnets, incorporated into a magnetic circuit, provide a radially directed magnetic field of which the strength is maximum in the vicinity of the channel exhaust. The magnetic field is chosen to be strong enough to make the electron Larmor radius much smaller than the discharge chamber characteristic dimensions, but weak enough not to affect ion trajectories. The electric potential drop is mostly concentrated in the final section of the channel owing to the low axial mobility of electrons in this restricted area. The electric field governs the propellant atoms ionization and the ion acceleration. The combination of the radial magnetic field with the axial electric field generates an E×B electron drift in the azimuthal direction, the so-called Hall current. The latter is responsible for the very efficient ionization of neutral atoms inside the channel.
The ISCT200 Hall thruster is a 200 W-class HT with a classical magnetic field topology, using xenon as propellant. Details about the ISCT200 series and thruster architecture can be found in [3, 15]. During operation, the thruster body is floating. A heated 5 A-class hollow cathode with a disk-shaped LaB_6 emitter was used to generate the electron current [23, 24]. The cathode is located outside the channel with its orifice in the vertical plane that contains the channel outlet, tilted towards the thruster. The cathode, which is operated with a constant xenon mass flow rate of 0.3 mg/s, is electrically connected to the thruster anode and floating. Note that the thruster plume slightly deviates from the the thruster axial direction, see figure 2. It results in a deviation of the ion beam measured by the FC as seen in figure 12.

The *ENPULSION NANO* is a $10 \times 10 \times 10$ cm^3 EP device engineered and produced by the company *Enpulsion GmbH* [12, 13, 25]. It is designed to be easily implemented into satellite structure. It is a 40 W-class thruster all systems included (i.e. heating, ion emission, neutralization). It is built from

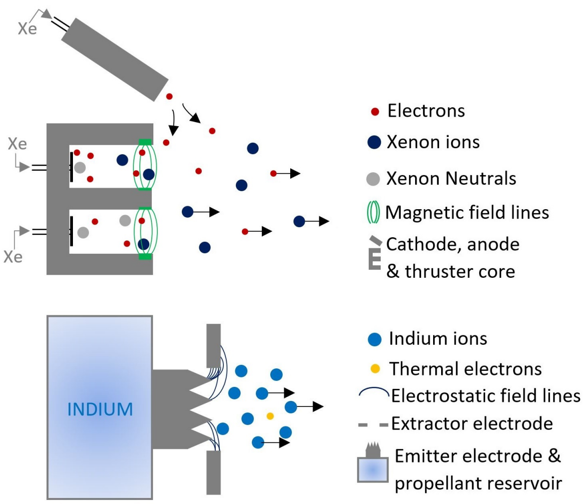

Figure 1: Working principle of the ISCT200 Hall thruster (top) and *ENPULSION NANO* FEEP (bottom). The ISCT200 uses xenon (Xe) as propellant while the *ENPULSION NANO* uses indium (In).

the heritage over 20 years of development done at *FOTEC GmbH* [26, 27, 28, 29, 2]. The thruster working principle is based on FEEP physics [30, 31, 32], see figure 1 (bottom). A strong electrostatic field (10^9 V/m) is applied at the tip of a porous, sharp and wetted structure [33, 34]. There, the surface is deformed and the fluid will turned into a cone-like structure as described by Sir Taylor [35]. The so called Taylor cone [36] permits to emit ionized particles from the tip of the wetted structure [37]. To provide E fields exceeding the emission threshold, called onset voltage, a counter electrode termed extractor is used. It aids in both ionization and acceleration process. It enables to reach electric fields exceeding 10 kV. The core of the *ENPULSION NANO* is a passively fed, porous ion emitter consisting of 28 sharp needle tips, also called injectors, see figure 2 (middle). The extractor is placed around the crown of needle to reach homogeneous fields. It is fuelled with indium. The molten metal can be used in its liquid states when the thruster reservoir is higher than 156.6°C. The thruster does not need cathodes to operate. The unit used in this experiment series is an *ENPULSION NANO* laboratory unit (ENP-LU), see figure 2 (right). The ENP-LU is operated with its own digitally controlled power processing unit (PPU) [25]. It allows accurate control and measurement of the emission voltage (V_{em}) and current (I_{em}). The ENP-LU fires with 16 well distributed injectors. The reduced amount of firing needles is due to the production process used on this laboratory unit [14]. It will result in a slight deviation of the ion beam to the positive side of the thruster angular distribution visible in figure 11.

The ENP-LU is operated in direct current control mode. Therefore, the ion current corresponds to the emission current measured on the PPU. To reduce uncertainties due to small current oscillations during operation ($\sim 1\%$), the so-called known ion current I_{em}, results from an average of emission

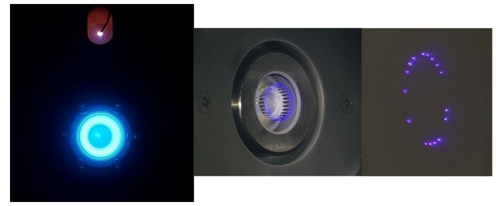

Figure 2: The ISCT200 (left), the ENPULSION NANO flight unit (middle) and its laboratory unit, ENP-LU (right), in operation.

Table 1: ISCT200 and ENP-LU operation points. Both thruster fire at constant current for different ion energies.

Thruster	I_{em} (mA)	V_{em} (V)
ENP-LU	2	5000
ENP-LU	2	6000
ENP-LU	2	7000
ENP-LU	2	8000
ENP-LU	2	9000

Thruster	I_d (A)	U_d (V)
ISCT200	0.66	200
ISCT200	0.66	250

current measured on the PPU over 800 s. In this manner, we can compare the experimental ion current $I_{i_{exp}}$ to I_{em} and determine the FC collection efficiency and reliability, see section 4.2 and 5.3. The ISCT200 is operated in current control mode as well. However, here the current corresponds to the discharge current I_d, which is the sum of the electrons and ion contribution to the current. Therefore, it is not possible to know the real ion current unless we use a reliable plasma diagnostic. Consequently, data obtained with ENP-LU will help to optimize the FC in order to accurately map the ISCT200 ion beam.

For both thrusters, all ion current measurements were done at constant emission current for different ion energies, see table 1. The ENP-LU was operated at 2 mA with emitter voltages (V_{em}) varying from 5 kV to 9 kV. The ISCT200 fired with a discharge current of 0.66 A and with U_d equals to 200 V and 250 V. Note that in the case of FEEP thruster, the acceleration voltage is assumed to be equal to the emitter potential and energy loss are not considered [29].

3 Faraday cup

3.1 Architecture

Measurements of the ion current density in the plasma plume or ion beam of electric propulsion devices is of great relevance as the flux of ejected ions determines the thruster properties such as the thrust level, beam divergence, the specific impulse, the propellant utilization and it plays a key role in thruster overall performances. Moreover, an accurate and comprehensive knowledge of this quantity is critical for the validation of plume modelling and numerical simulations, for thruster acceptance tests, for the study of facility effects and for understanding the interactions between plasma plume and spacecraft elements. A Faraday Cup (FC) is a special kind of electrostatic planar probe. It is basically an isolated conductive cup dedicated to the detection of charged particles in a low-pressure or vacuum environment [1]. When a Faraday cup operates as an ion collector, which means the cup is negatively biased with respect to the floating potential, the ion current in the probe direction can be accurately measured. Contrary to other electrostatic probes, edge effects due to plasma sheath formation are negligible with a FC owing to the closed geometry.

In this study all Faraday cup configurations share a common base architecture showed in figure 3. The pod or housing (4) is grounded and shields the electrodes from the ambient plasma. It is electrically isolated, with PEEK material, from any conductive part of the probe. Inside, the collimator electrode (3) is used to define the ion flux going through the diagnostic. Hence, it needs to have the smallest area of the system. It screens electrons and acts as a filter for ion velocity vector. In this manner, it avoids saturation of the measurement chain when the FC is placed in the centre of the ion beam. Moreover, it helps to minimize CEX effect on the FC output [38]. It is the most exposed part to the ion beam. Then, it needs to support high level of stress such as local heating, pulverization, deposition. The collimator sits right behind the housing front. To minimize confusion between collector and collimator electrodes, the latter will be termed repeller in the next sections. Finally, the collector electrode, composed of a disk and a cup (1+2), is used to collects the collimated ion flux. The collector is subject to heavy ion bombardment and sensitive to the resulting ion induced electron emission. The collector material property and geometry are not part of the study. Based on different studies which aimed to enhance ion collection and minimize SEE events [39, 40, 41, 42, 43], the collector diameter is fixed to 12 mm and the bottom of the cup is a AlSi7Mg open-cell foam disk (Nr.4) provided by Exxentis [44]. Note that IIEE are minimized but not suppressed with such collector properties. PEEK insulators (5) are used to prevent electrical connection between these three components.

Figure 3 shows as well the different architectures studied in this work. To enable a good comprehension through this study a nomenclature (ID) is used to identify all Faraday cup designs. Each ID is split in four components and can be found as X.X.X. The first label refers to the material facing the beam used in front of the probe. It can be either *graphite* (G), *molybdenum* (Mo) or *aluminium* (Al). Then, the second one informs on the inlet aperture diameter. It can be 10, 07, 05, 03 or 01 mm. Finally, the third label gives information upon the position of the collimator electrode. If the repeller is exposed to the ion beam and collimates the ion flux, then the letter E is used. On the contrary, in the case the repeller is placed behind the housing, and the pod front aperture d_{pod} is smaller

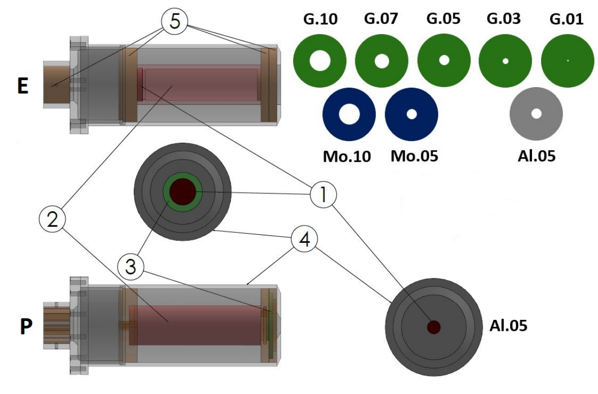

Figure 3: 3D model of all Faraday cup designs tested

than the repeller one d_r, the repeller is considered protected from the ion beam, then the letter P is used. For example, the FC identified as G.07.E refers to a Faraday cup where the part of the probe facing the ion beam is graphite, the opening diameter is 7 mm and the collimator is in the configuration where it is exposed to the plasma. Furthermore, a FC called Al.05.P has its front material in aluminium, its aperture is 5 mm and the collimator is in a "protection" configuration.

3.2 Perturbations

Using a Faraday cup to assess beam properties of an EP device generates plasma - probe interactions. They might disturb and corrupt the data obtained with the plasma diagnostic. The material (housing, collimator and collector) undergoes important level of stress when bombarded with highly energetic ions. In such conditions any material might experience three phenomena: Ions rebound or reflection, atoms (i.e Neutral) sputtering and ion induced electron emission (IIEE). The latter is the most critical.

Secondary or ion induced electron emission (IIEE) are the predominant perturbation during ion current measurements with a Faraday cup. Once the primary ion is collected an electron can be ripped off the target surface and ejected. Consequently, the measured ion current $I_{i_{exp}}$ is artificially increased and reads $I_{i_{exp}} + I_{IIEE}$, with I_{IIEE} the current contribution of ion induced electrons. It is related to the ion current $I_{i_{exp}}$ with $I_{IIEE} = \gamma_{IIEE} \times I_{i_{exp}}$. The factor γ_{IIEE} informs on the capacity of a material to retain secondary electron emissions. The lower the yield the more efficient the material. There are two possibilities to minimize the effect of IIEE on the measured ion current. On the one hand, one can optimize the cup geometry (length, form) of the FC to increase the probability to recapture secondary electrons. On the other hand, one can use different potential field lines inside the cup to redirect secondary electrons back to the collector and completely suppress the IIEE effect. The second option is studied in this work and introduced in section 5.2.

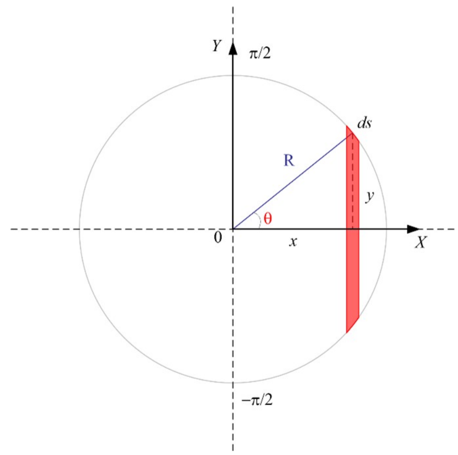

Figure 4: Schematic of the cylindrical coordinate system used to compute the experimental ion current $I_{i_{exp}}$ from the current density angular distribution profile.

4 Ion current

4.1 Total ion current $I_{i_{exp}}$

The ion current $I_{i_{exp}}$ corresponds to a flux of positive charges going through a surface per unit of time. It is expressed in A [C/s]. It reads:

$$I_{i_{exp}} = \int\int j_i dS. \tag{1}$$

The ion current density j_i (A/m^2) is here assumed to be collinear to the outward pointed unit normal vector to the surface. A spherical coordinate system is often used to determine dS and compute $I_{i_{exp}}$. The probe is usually fixed at a distance R and the thruster is supposed to be a point source at the centre of a sphere. To compute $I_{i_{exp}}$ it is needed to know $j_i(\theta,\phi)$, where θ is the latitude and ϕ the longitude. When the current density is solely recorded in a plane that contains the thruster axis, e.g. following the angle θ from $-\pi/2$ to $\pi/2$, one can assume a cylindrical symmetry of the ion beam around the thruster axis to determine $j_i(\theta,\phi)$ and compute $I_{i_{exp}}$. It is in fact easier to use a cylindrical coordinate system to solve equation 1. In that case the coordinate system is depicted in figure 4 along with the elementary arc ds. The thruster exit plan points toward the x axis. Measurements are performed at a fixed distance R and defined by the angle θ. Cylindrical symmetry implies a constant j_i inside the element with radius y and thickness ds. The sum of these elements, each weighted with $j_i(\theta)$, gives the ion current:

$$I_{i_{exp}} = \int_0^R j(x,y) 2\pi y ds, \tag{2}$$

with $j_i(x,y) = j_i(\theta)$. With the help of several mathematical convention and simplification we obtain the general final form of the ion current [45]:

$$I_{i_{exp}} = 2\pi R^2 \int_0^{\frac{\pi}{2}} j_i(\theta)\sin(\theta) d\theta. \tag{3}$$

This form is also used by Brown et al. [18] in his recommended guidelines for use of Faraday probes. In the case of perfect symmetry around the x axis we can use the form proposed in equation 3. If the ion beam is not symmetric, one must use an integral from $-\pi/2$ to $\pi/2$. Therefore, equation 3 is split into the sum of two terms that represents positive and negative angles:

$$I_{i_{exp}} = \pi R^2 \left[\int_0^{\frac{\pi}{2}} j_i(\theta)\sin(\theta) d\theta + \int_0^{\frac{-\pi}{2}} j_i(\theta')\sin(\theta') d\theta' \right]. \tag{4}$$

This comes down to take the absolute of the sinus inside the integral as followed:

$$I_{i_{exp}} = \pi R^2 \int_{\frac{\pi}{2}}^{\frac{\pi}{2}} j_i(\theta) \mid \sin(\theta) \mid d\theta. \tag{5}$$

4.2 Probe efficiency

The probe efficiency of the Faraday cup (η_p) is used to evaluate and compare FC designs between each other. As explained in section 2.2, the ENP-LU thruster is operated in direct emission current mode. Therefore the measured experimental ion current $I_{i_{exp}}$ should ideally be equal to the emitted ion current I_{em}. η_p corresponds to the ratio between these two values and it reads:

$$\eta_p = \frac{I_{i_{exp}}}{I_{em}}. \tag{6}$$

For a perfect collection efficiency the ratio equals 1. In reality systematic errors only allow to have an experimental ion current approximately equal to the known emitted current. Therefore, the goal is to optimize the FC design to bring η_p close to 1 as expressed in equation 6.

4.3 Beam divergence

The divergence half-angle θ_{div} refers to the width of the beam. It quantifies the beam deviation from a straight ion beam. The thrust is directly impacted and it significantly decreases when the divergence angle gets large. The divergence half-angle θ_{div} of the ion beam is defined as the angle for which the ion current corresponds to a given fraction of the total ion current. In general, the ratio is 0.95. Therefore, the half-angle is mathematically related to I_i according to:

$$I_{i_{\theta_{div}}} = \pi r^2 \int_0^{\theta_{div}} j_i(\theta) \cdot \sin(\theta) \cdot d\theta = 0.95 \cdot I_{i_{exp}}. \tag{7}$$

Equation 7 shows that the way $I_{i_{exp}}$ is calculated, as well as the treatment of the angular distribution of the ion current density (smoothing, fitting, filtering, interpolation), greatly influence the value of θ_{div} for a given dataset. Appropriate design of a FC must reduce at maximum the need for data processing.

4.4 Current and propellant utilization

The current utilization (η_b) is of importance for Hall thrusters as those devices are not operated with direct ion current control. A Hall thruster provides thrust when delivering a discharge current (I_d) that incorporates both ion and electron contribution. The current utilization is the ratio between the experimental ion current and I_d.

$$\eta_b = \frac{I_{i_{exp}}}{I_d}. \tag{8}$$

This ratio is around 0.8 for HTs [3, 46]. That means about 20% of the current is produced by electrons which do not contribute to the thrust.
The propellant utilization α is the ratio of the ion mass flow rate to the propellant mass flow rate. It corresponds to the fraction of the propellant mass flow rate injected into the discharge channel that is ionized. This quantity directly characterizes the ionization efficiency, hence it has to be maximized. Note that multiply-charged xenon ions with charges up to 5+ have been detected in the plume of high-power Hall thrusters. As the multiply-charged ion fraction is often unknown, the ion beam is assumed to be solely composed of singly-charged ions. The propellant utilization reads [47, 48]:

$$\alpha = \frac{1}{\dot{m}} \frac{I_{i_{exp}}}{e} m. \tag{9}$$

Where $\dot{m}$ is the propellant mass flow rate, m is the atomic mass, e is the elementary charge and $I_{i_{exp}}$ the experimental ion current. In all cases accurate FC measurements are used to get more precise and reliable values for the current ionization as this quantity plays a key role in HT optimization.

5 Faraday cup characteristics

5.1 Faraday cup beam exposure

Often, Faraday cups equipped with a repeller [38, 1, 2] are similar to configuration X.X.E where the repeller is directly exposed to the plasma. Therefore, this electrode undergoes high level of stress (local heating, sputtering, IIEE) which can corrupt the data measured by the collector sitting right behind. Moreover, the Faraday cup principle relies on the good insulation of its collector, collimator and housing. Therefore, using a design where the repeller is exposed to the beam increase the probability to create a short-circuit between two electrodes after a long time of operation as pictured in figure 5. The left side of the photograph shows the front of a FC in configuration X.X.E after operation under indium ion bombardment. The PEEK insulator which electrically separates the repeller from the housing sits behind the housing front. The right side shows indium deposition on this PEEK insulator. We observe the absence of deposition on the part of the probe constantly

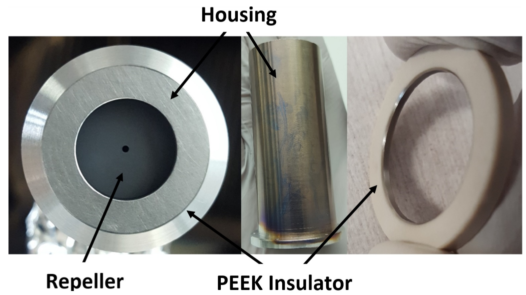

Figure 5: Faraday cup front cleanness (left) and Indium deposition on PEEK insulator (right) observed on Faraday cup configuration X.X.E after being exposed to the highly energetic ion beam of the ENP-LU.

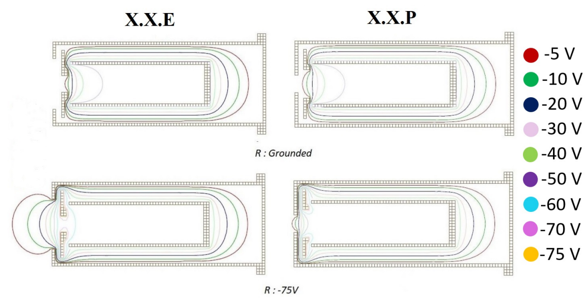

Figure 6: Numerical simulation of the potential filed lines inside a Faraday cup obtained with the software SIMION.

exposed to the ion beam. However, parts which are never directly exposed to the plume show propellant deposition (side part of the probe and PEEK insulator). Using the configuration X.X.P will prevent any deposition inside the Faraday cup. Note that specific care must be taken on the material chosen to equip the FC front, see section 5.4, as it will now be used to collimate the ion flux going through the cup.
Additionally, Ion beams examined in this study cover a wide energy range, 10 eV to 10000 eV. One must minimize the perturbation to the plasma plume induced by potential field lines due to voltage applied to the cup electrodes. An academic version of the software SIMION is used to simulate the field lines created by the cup when different potential are applied. SIMION is a simulation program that models ion optics problems. Two Faraday cup configurations (X.X.E and X.X.P) are presented in figure 6. For each configuration the collector potential is set to -50 V while the repeller is either kept grounded (top) or bias to -75 V (bottom). For both configurations the filed lines are confined inside the Faraday cup when the repeller is grounded. However, when a potential is applied on the repeller the field lines created are completely invading the vicinity of the probe with the configuration X.X.E while they are kept confined with the other design. The larger the potential the more the intrusion. As we want to study the effect of modifying the electric field inside the probe to minimize IIEE effects the configuration X.X.P seems preferable to use.

5.2 I-V curves

Prior to experimental ion current determination, current-voltage (I-V) characteristic curves must be acquired to verify the proper design and functioning of the probe. An I-V curve consists of a potential sweep on the Faraday cup collector at different angular position in the EP plume. The sweep goes from negative to positive value. When the collector is negatively bias, the probe collects ions and the so-called ion branch can be measured and quantify. On the positive side of the I-V curve, the current measured refers to the electronic branch. There, one can determines plasma and electron properties such as plasma and floating potentials as well as electron density and temperature. In this work we will focus on the ion branch of an I-V curve.

Upstream geometry optimization, we assess the feasibility to modify the electric field inside the Faraday cup to minimize or suppress ion perturbation such as IIEE (section 3.2). Therefore, I-V curves for different repeller potentials have been acquired within the ENP-LU and ISCT200 plasma plumes, see figure 7. Measurement are acquired with the Faraday cup configuration Al.05.P to reduce field perturbation in the plasma vicinity. There, the repeller is either grounded or biased to -20 V, -25 V, -50 V, -75 V or -100 V while the collector potential is swept from -180 V to 10 V. The current density measured on both thruster axis (i.e. 0°) is express in μA/cm^2 and mA/cm^2 for the ENP-LU and ISCT200 respectively. In figure 7 we observe two different behaviours. The top plot shows the ion branch measured with the ENP-LU while the bottom one displays measurement done with the ISCT200. The modification of repeller potential does not impact the ion branch amplitude measured on the ENP-LU. In contrast, for the ISCT200 Hall thruster, one can note the diminution of ion current measured by the FC collector when the repeller potential is biased more negatively. The ENP-LU operates with ion energies of the order of its acceleration potential (i.e. several kV) [29], therefore, they are not affected by the weak potential field lines created inside the probe. Similarly, ions travelling within the ISCT200 beam can't excess its discharge voltage which is only in the order of few hundreds volts (i.e 250 V). Moreover, the ion energy distribution of a HT is large [3] compared to the beam of a FEEP thruster [29]. Consequently, the velocity vector of those ions is subject to perturbations when an electric field is created in its vicinity. Ions not captured by the probe collector are instead attracted by the repeller.

Figure 8 shows two I-V curves from the ENP-LU when operated at 2 mA with ion energies in the order of 7 keV. The plot located at the top of the figure represents a current measured by the collector. The second plot, displays a current measured on the repeller. Both curves are acquired simultaneously when the collector potential is swept from -180 V to 10 V and the repeller potential (V_r) is fixed at -100 V. First of all, we note that both currents are positive which reflect ions collection on both electrode. Nevertheless, the ion current seen on the repeller corresponds to maximum ~5% of the ion current measured by the collector. Secondly, it is seen that both I-Vs can be separated in three zones. Zone 1 shows current obtained when the collector potential is lower than the repeller one ($V_c < V_r$). There, the ion induced electron emitted by the collector are attracted by the repeller potential, hence increasing the current seen on the collector. Then, zone 2 represents the current acquired once the collector voltage overtakes the repeller one ($V_r < V_c$). Note that in zone 2 both electrodes are still negatively biased. Here, IIE which were lost in zone 1 are now redirected toward the collector, then properly recollected. The IIE recollection is represented by a current drop on the collector and a current increase on the repeller. Finally, zone 3 shows ion current acquired when the collector voltage is positive. Another current drop is observed on the collector while an important increase is seen on the repeller current. In this zone the collector is now capturing thermal electrons from the ambient plasma and IIE created by the probe front. The repeller current measured in zone 3 is three times higher than the one seen in zone 2. This shows the importance of shielding the collector from ambient electrons. Consequently, in the case of FEEP thrusters, the collector FC should be biased negatively to properly screen thermal and secondary electron present in the probe vicinity. Its potential should be greater than the repeller one to recollect all secondary electrons from the collector. Therefore, zone 2 is the appropriate area to set the FC to compute the total ion current delivered by the thruster. In the case of Hall thrusters, the working principle of such thrusters does not allow to use strong electric fields to recapture IIE. Moreover, zone 3 cannot be used as well since primary electrons are travelling along with ions. Additionally, since no current drop is observed on I-V curves measured on the ISCT200 axis, see figure 7, one can agree that the length of the cup (50 mm) is long enough to recollect all IIE. Therefore, zone 1 is preferable to measure the ion current of these EP devices.

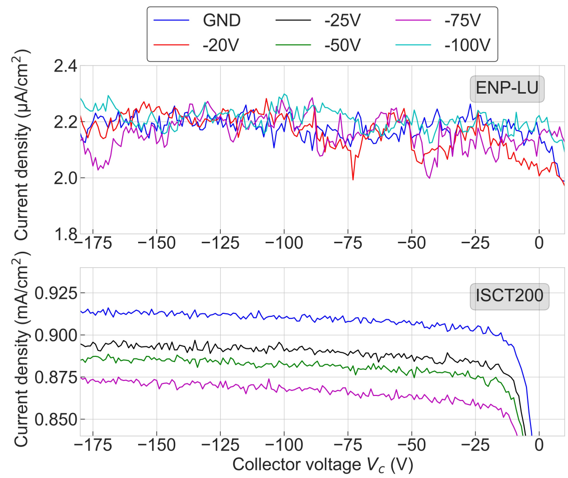

Figure 7: Ion branch of I-V curves from the ENP-LU thruster (top) and the ISCT200 Hall thruster (bottom). In both plot the electric field inside the Faraday cup is modified.

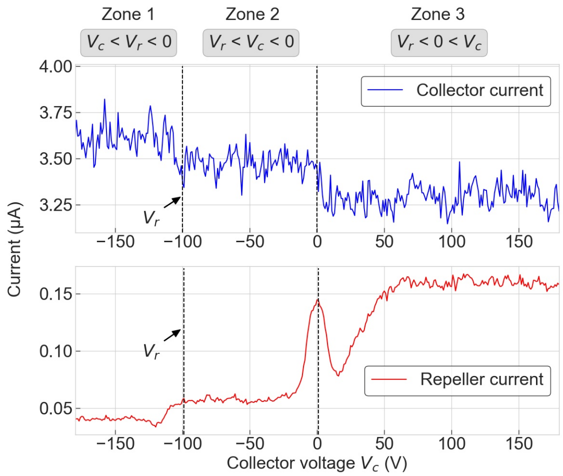

Figure 8: Determination of appropriate Faraday cup settings to measure and compute the experimental ion current of an electric thruster plume.

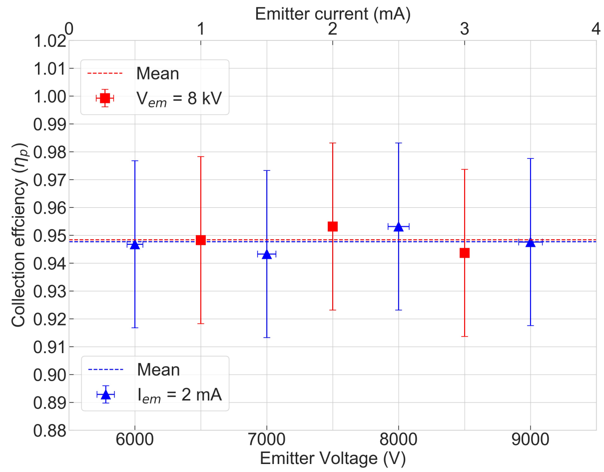

Figure 9: Faraday cup Al.05.P ion collection efficiency obtained from current density angular distribution of the ENP-LU plume.

5.3 Faraday cup accuracy and reliability

Data obtained with a Faraday cup is mainly influenced by the energy of ions travelling within the thruster plume. To a certain extent the ion density which characterizes the population of ions per unit of area can impact the FC output as well. To enable reliable thruster performance characteristics one must show the robustness of a FC design against ion energy and density perturbations. To this end, we first operated the ENP-LU at 2 mA of current emission (I_{em}) with acceleration potential (V_{em}) from 5 kV to 9 kV. Secondly, we set (V_{em}) to 8 kV while I_{em} was fixed to 1, 2 and 3 mA. For each firing configuration a plume scan was performed as described in section 2.1. The Faraday cup was in configuration Al.05.P. Figure 9 displays the probe efficiency (η_p), computed as described in section 4.2, for each firing operation. The blue colour represent efficiencies obtained when the thruster fires at constant current while the red colour concerns efficiencies computed at equal acceleration potential. First, we observe that η_p is stable for both constant current and voltage thruster operation. Moreover, the standard deviation between each η_p computed is less than 0.5%. Additionally, we note that with this Faraday cup design the probe is able to collect $\sim 95\%$ of the ion current from the thruster plume. Both data set give a collection efficiency average of $94.5 \pm 3\%$.

From these results we can argue that the Faraday cup design enable to measure more than 95% of the real ion current with a degree of confidence below 5%. Moreover, figure 9 proves the reliability and robustness of the FC ion collection for different current densities and ion energies.

5.4 Faraday cup front material

As explained in section 5.1 the front part of a Faraday cup is the most exposed to direct ion and electron impact. Therefore, the material must be able to withstand high level of stress. In the case of low power (≤ 200 W) EP devices, heat load experienced by the plasma diagnostic is less important than with high power electric thruster. Nevertheless, low power thrusters still carry energetic ions within their plume making these stresses not negligible. We assessed the impact of the material used to equip the front of a Faraday cup. Firstly, we used the Faraday cup configurations G.05.E, M.05.E and Al.05.E for the ENP-LU. For the ISCT200 configurations G.10.E and Mo.10.E were tested. The first plot displayed in figure 10 represents the ion collection efficiency obtained with the ENP-LU. On the second plot the current and propellant utilization for the ISCT200 are shown. For the FEEP thruster efficiency decreases when the probe front is made of molybdenum. It drops even more with aluminium. We observe a decrease for the current and propellant utilization in the case of the HT when the FC is equipped with Mo. As explained in section 4.4, these two parameters depend directly on the ion current measured. For a given FC design both parameters are computed with only a modification of $I_{i_{exp}}$. Therefore, a variation on these figures would induces a variation of the ion current collected. For the FEEP thruster we note a maximum variation of 6% in collection efficiency between FC configuration. In contrast, η_b and α can drop by by 14% and 12.5% respectively in the case of the HT. The third plot in figure 10 displays η_p (FEEP), η_b (HT) and α (HT) obtained with FC configurations X.X.E and X.X.P. In the case of the FEEP (red), we compared the probe ion collection efficiency between FC configuration Al.05.E and Al.05.P, where the material facing the plume is identical (aluminium). We observe that the efficiency increases when the FC is in configuration

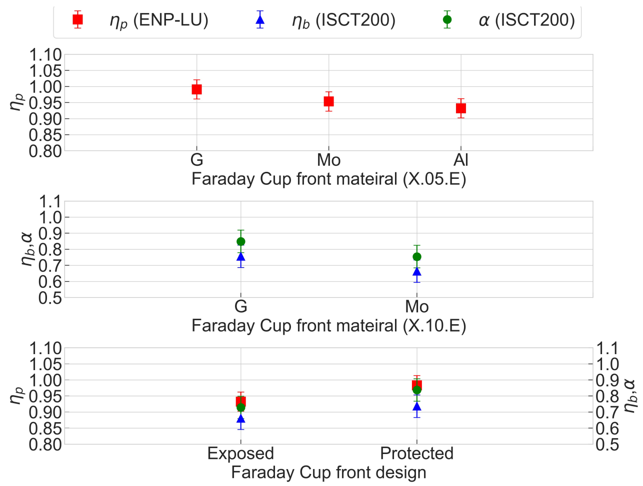

Figure 10: Evolution of the normalized ion current measured on the ENP-LU and ISCT200 plume with different FC configuration.

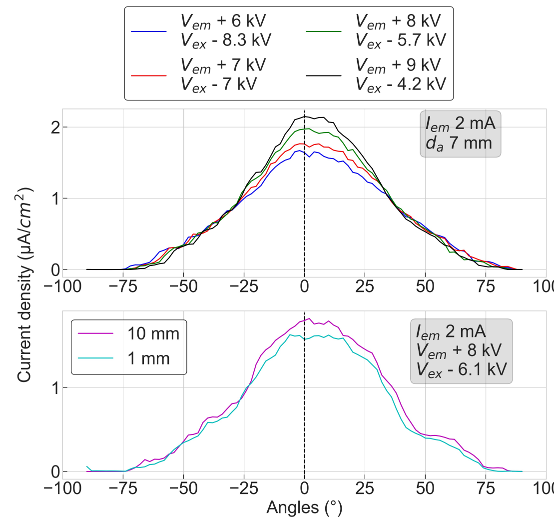

Figure 11: Current density profiles of the *ENPULSION NANO* laboratory unit for different thruster operating points (top) and aperture diameters of 10 mm and 1 mm (bottom).

X.X.P. In the same manner, the current (blue) and propellant utilization (green) computed with configuration G.05.E and AL.05.P are plotted as well. The same behaviour is observed. Note that with the X.X.P configuration the top of the collector cup is further away from the probe entrance since we use the front of the probe, not the repeller, to collimate the ion flux. Therefore, the distance between the ambient plasma and the collector increases by few millimetres. Moreover, with configuration X.X.P the repeller is physically shielding the collector from undesirable particle created by the probe front.

Results presented in this section reinforce the analysis done in section 5.1. A Faraday cup in a configuration where the housing front collimates the ion flux while a secondary electrode called repeller is placed behind, and protected from direct ion impact, increases the accuracy and reliability of the probe ion collection.

5.5 Faraday cup front aperture

The aperture diameter of a Faraday cup is of great importance as it defines the collection area used to obtain the ion current density. Faraday cup configurations G.01.E, G.03.E, G.05.E, G.07.E and G.10.E were used to measure the angular ion current density distribution of the ENP-LU (figure 11) and ISCT200 plume (figure 12). The first plot in figure 11 displays the ion beam profiles of the ENP-LU for different ion energy and constant current emission (2 mA) for a given FC configuration (G.07.E). In order to keep I_{em} constant for different acceleration potential, the extractor potential (V_{ex}) must ba adjusted which modified the beam width. The smaller V_{ex} the more focus the ion beam. It results with higher current densities measured on the thruster axis and less at the thruster wings. We know from section 5.3 that it does not impact the ion collection efficiency of the probe, therefore the experimental ion current will be identical in all cases. The second plot (bottom) in figure 11 shows the ion beam shape at constant current and voltage emission acquired with configuration G.10.E and G.01.E. The latter reads less current density on the thruster axis. Figure 12 displays the ion beam profile of the ISCT200 Hall thruster plume firing at 0.66 A with 200 V (top) and 250 V (bottom). Once more the intensity of the ion current density decreases with the aperture diameter of the probe with a major drop when $d_a < 5$ mm. On the face of it, the relation between the angular current density distribution and the aperture diameter of the Faraday cup looks more important in the case of a Hall thruster than for a FEEP.

From the beam profiles showed in figure 11 and 12 the ion current is computed. Figure 13 presents the values obtained for η_p (red) with the ENP-LU, η_b (blue) and α (green) with the ISCT200. In the case of the ENP-LU we observe a small decrease of the collection efficiency when the diameter is reduced. Almost no differences are noticed between 10 mm and 7 mm as well as between 5 mm and 3 mm. Overall, η_p decreases by 5% when d_a is reduced by a factor 2 and by 10% when reduced by 10. For the ISCT200, the ion collection losses of the Faraday cup is even more visible and pronounced. η_b and α can drop by ∼10% if d_a decreases by a factor 2 and by ∼50% if decreased by 10. Note that the front of a Faraday cup also acts as an ion velocity vector filter. It means reducing the probe aperture increases ions selection with directions collinear to the probe axis to reach the collector. Moreover, for smaller aperture diameter, the probe alignment requires more accuracy when performed. The uncertainty and possible error will increase and be added to the ion selection process which strengthen the losses to the ion collection. The major drop of η_p in the case of the ISCT200 could be explained by the invalidity of the point source assumption, for a given collection surface, that is often found in the literature. Ions originate from an extended region of space

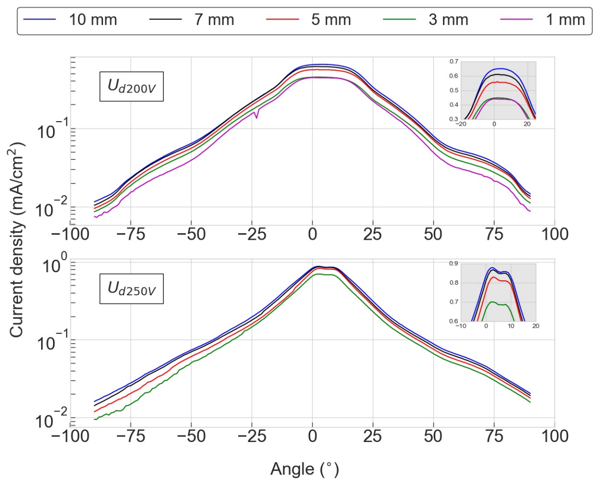

Figure 12: Current density profiles of the ISCT200 Hall thruster measured for discharge voltages of 200 V (top) and 250 V (bottom) and constant I_d with different FC aperture diameters.

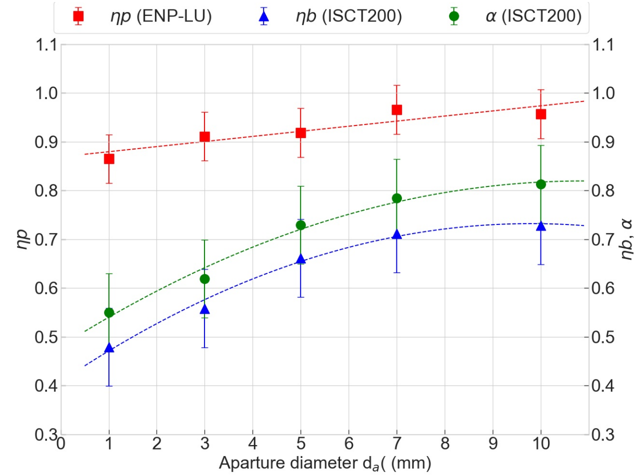

Figure 13: Impact of the aperture diameter of a Faraday cup upon the computation of the ion current in the case of a FEEP thruster (top) and Hall thruster (bottom). The lines are here to guide the eyes.

that has an annular geometry. Moreover, the velocity vector dispersion is large in the case of Hall thrusters due to the overlap between the ionization and acceleration zones combined with many scattering and charge exchange collision events. These phenomena are strongly reduced or even absent from a FEEP plume as it mainly consists of an ion beam where ionization and ion acceleration are localized on a small region and happen one after the other. For those reasons the collected ion current strongly depends on the FC aperture dimensions. Note that this work reveals the thruster to probe distance necessary for the point source assumption to be valid is much longer than 4 thruster diameters, a classical value often encountered, when the probe aperture diameter is lower than 5 mm.

Finally, in the same manner than the collection efficiency, the divergence angle θ_{div} computed for each aperture diameter is plotted in Figure 14. This parameter can be influenced by the extractor potential and the mas flow rate for the ENP-LU and the ISCT200 respectively. Therefore, for each data point the entire controllable firing conditions for each EP device are plotted. On the opposite of η_p, it is clearly seen that θ_{div} is not impacted by the value of the Faraday cup collection area. One could argue that the ratio of ions missed by the collector probe is constant over the entire angular distribution profile.

6 Conclusion

In this study we compared for the first time the effect of a Faraday cup design upon the determination of crucial plume parameters such as ion current, beam divergence, current and propellant utilization. The focus was on the impact of the Faraday cup front architecture. The work revealed that the efficiency of ion collection of an electric thruster plume, independently from its specific operation characteristic, can be optimized if one uses the right materials, aperture dimensions and operate the probe with the right potentials.

Moreover, we compared the output obtained with two different EP technologies namely a Hall Thruster and a FEEP thruster. These two thrusters differ in many points such as propellant, beam current density and ion energy. It appeared that despite their differences similar behaviours are observed when the same plasma diagnostic is used to study their beam. Indeed, for a FC configuration where the repeller is exposed to the plume, the material used is of great importance. It is preferable to use a material with low sputtering yield and weakly impacted by secondary electron emission. Using a design where the front of the probe housing collimates the ion flux and the repeller is placed behind and protected from direct ion impact increases the probe reliability. In this manner, the probe is shielded against particle deposition and its potential field lines do not penetrate the ambient plasma in the probe vicinity. Additionally, it prevents background particles and undesirable ones to travel through the collector electrode and disturb the collected current.

Nevertheless, despite their similarities some design parameters are more impacted depending on the EP device studied. For EP devices operating with highly energetic ions, the probe needs to be operated with specific potential applied to all electrodes. The collector and repeller need to be negatively biased with $V_r < V_c$. This way, all secondary electrons are recollected. In the case of EP devices firing with lower are more disperse ion energy, the repeller should be left grounded while only the collector is negatively biased. For these thrusters only the probe architecture can be optimized to recollect the IIE. Finally, the ion collection efficiency strongly depends on the probe aperture diameter, for a given thruster-to-probe distance. We observed that for distances larger than 15 times the thruster mean diameter the relation between the experimental ion current and probe entrance diameter is drastically reduced.

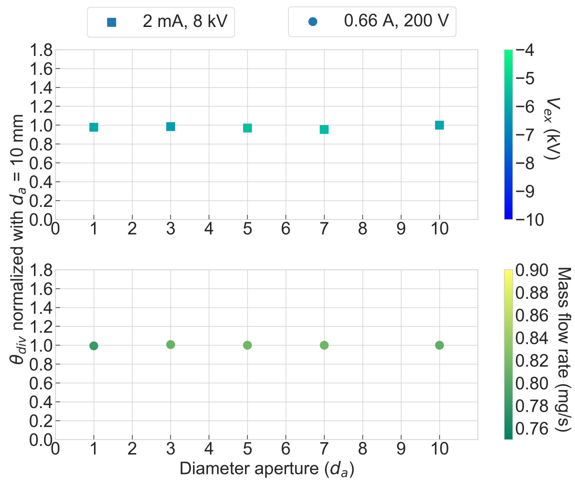

Figure 14: Impact of the aperture diameter of a Faraday cup upon the determination of the divergence angle θ_{div} in the case of a FEEP thruster (top) and Hall thruster (bottom)

To improve plasma diagnostic standardization and reliability further studies should be carried out on the relation between the Faraday cup collector material and geometry with the ion collection efficiency.

References

[1] S.Mazouffre, G.Largeau, L.Garrigues, C.Boniface, and K.Dannenmayer. Evaluation of various probe designs for measuring the ion current density in a Hall thruster plume. In *35th International Electric Propulsion Conference*, October 2017.

[2] S.Keerl, W.Engel, N.S.Mühlich, J.Fries, and B.Seifert. Two-dimensional plasma plume density characterisation of the IFM Nano Thruster. In *36th International Electric Propulsion Conference*, September 2019.

[3] T.Hallouin and S.Mazouffre. Far-Field Plume Characterization of a 100-W Class Hall Thruster. *Aerospace*, May 2020.

[4] L.Habl, D.Rafalskyi, and T.Lafleur. Ion beam diagnostic for the assessment of miniaturized electric propulsion systems. *Review of Scientific Instruments*, 2020.

[5] D.Selva and D.krejci. A survey and assessment of the capabilities of Cubesats for Earth observation. *Acta Astronautica*, 74, 2012.

[6] J.N.Pelton, S.Madry, and S.Camacho-Lara. *Handbook of Satellite Applications*. Springer edition, 2017.

[7] A.W.Hanson. Satellite Internet in the Mobile Age. *New Space*, 4, 09 2016.

[8] D.M.Goebel and I.Katz. *Fundamentals of Electric Propulsion: Ion and Hall Thrusters*. Jet propulsion laboratory, california institute of technology edition, 2008.

[9] S.Mazouffre. Electric propulsion for satellites and spacecraft: established technologies and novel approaches. *Plasma Sources Science and Technology*, 25(3):27, April 2016.

[10] K.Lemmer. Propulsion for CubeSats. *Acta Astronautica*, 134, 2017.

[11] D.Krejci and P.Lozano. Space Propulsion Technology for Small Spacecraft. In *Proceedings of the IEEE*. IEEE, 2018.

[12] A.Reissner, N.Buldrini, B.Seifert, T.Hörbe, and F.Plesescu. Testing and Modelling of the mN-FEEP Start-Up Performance. In *34th International Electric Propulsion Conference*, July 2015.

[13] D.Krejci and A.Reissner and T.Schoenherr and B.Seifert and Z.Saleem and R.Alejos. Recent flight data from IFM Nano Thrusters in a low earth orbit. In *36th International Electric Propulsion Conference*, September 2019.

[14] T.Schoenherr and B.Little and D.Krejci and A.Reissner and B.Seifert. Development, Production, and Testing of the IFM Nano FEEP Thruster. In *36th International Electric Propulsion Conference*, September 2019.

[15] S.Mazouffre, G.Bourgeois, K.Dannenmayer, and A.Lejeune. Ionization and acceleration processes in a small, variable channel width, permanent-magnet Hall thruster. *Journal of Physics D: Applied Physics*, 45(185203), April 2012.

[16] L.Grimaud. Magnetic shielding topology applied to low power Hall Thrusters, October 2018.

[17] J.Vaudolon. Electric field determination and magnetic topology optimization in Hall thrusters, October 2015.

[18] D.L.Brown, M.L.R.Walker, J.Szabo, W.Huang, and J.E.Foster. Recommended Practice for Use of Faraday Probes in Electric Propulsion Testing. *Journal of Propulsion and Power*, 33(3), May - June 2017.

[19] D.L.Brown and A.D.Gallimore. Evaluation of ion collection area in Faraday probes. *Rev. Sci. Instrum.*, 81:063504, 2010.

[20] D.L.Brown and A.D.Gallimore. Evaluation of facility effects on ion migration in a Hall thruster plume. *J. Propul. Power*, 27:573–585, 2011.

[21] S.Humphries. Intense ion-beam neutralization in free space. *Applied Physics Letters*, 32, 1978.

[22] V.V.Zhurin, H.R.Kaufman, and R.S.Robinson. Physics of closed drift thrusters. *Plasma Sources Sci. Technol*, 8, 1999.

[23] R.Joussot, L.Grimaud, and S.Mazouffre. Examination of a 5 A-class cathode with a LaB_6 flat disk emitter in the 2 A - 20 A current range. 146:10, 2017.

[24] G-C.Potrivitu, R.Joussot, and S.Mazouffre. Anode position influence on discharge modes of a LaB_6 cathode in diode configuration. *Vacuum*, 151:122–132, February 2018.

[25] D.Krejci, V.Hugonnaud, T.Schönherr, B.Little, A.Reissner, Q.Koch, E.Bosch Borràs, and J.González Del Amo. Full Performance Mapping of the IFM Nano Thruster including Direct Thrust Measurements. *Journal of Small Satellites*, 8(2):881–893, 2019.

[26] I.Vasiljevich, M.Tajmar, W.Grienauer, F.Plesescu, N.Buldrini, J.Gonzalez Del Amo, B.Carnicero-Dominguez, and M.Betto. Development of an Indium mN-FEEP Thruster. In *44th AIAA/ASME/SAE/ASEE Joint Propulsion Conference and Exhibit*, July 2008.

[27] R.Sypniewski Richard N.Buldrini A.Reissner D.Jelem, B.Seifert. Performance mapping and qualification of the IFM Nano thruster EM for in orbit demonstration. In *53rd AIAA/SAE/ASEE Joint Propulsion Conference*, October 2017.

[28] D.Jelem, A.Reissner, B.Seifert, N.Buldrini, L.Wilding, and D.Krejci. Direct thrust and plume divergence measurements of the IFM Nano Thruster. *Advances in Space Research*, 62(12):3398–3404, 2018.

[29] N.Mühlich, S.Keerl, W.Engel, E.Ceribas, and R-J.Koopmans. Retarding Potential Analyser Development for Low Density FEEP Thruster Beam Diagnostics. In *36th International Electric Propulsion Conference*, September 2019.

[30] S.Marcuccio, A.Genovese, and M.Andrenucci. Experimental Performance of Field Emission Microthrusters. *Journal of Propulsion and Power*, 14(5), 1998.

[31] A. Genovese, W.Steiger, and M. Tajmar. Indium FEEP microthruster: Experimental characterization in the 1-100μN range. In *37th AIAA/ASME/SAE/ASEE Joint Propulsion Conference and Exhibit*, July 2001.

[32] M.Tajmar, A.Genovese, and W.Steiger. Experimental Performance of Field Emiision Microthrusters. *Journal of Propulsion and Power*, 20(2), 2004.

[33] A.Genovese, N.Buldrini, M.Tajmar, E.Tamas, I.Vasiljevich, and K.Marhold. Development of an Indium mN-FEEP Thruster. In *41st AIAA/ASME/SAE/ASEE Joint Propulsion Conference and Exhibit*, July 2005.

[34] I.Vasiljevich, N.Buldrini, F.Plesescu, M.Tajmar, M.Betto, and J.Gonzalez Del Amo. Porous Tungsten Crown Multiemitter Testing Programmes Usin Three Different Grain SIzes and Sintering Procedures. In *The 32nd International Electric Propulsion Conference*, September 2011.

[35] G.I.Taylor. Desintegration of water drops in an electric field. *Royal Society*, 280, 1964.

[36] J.F.De La Mora and I.G. Loscertales. The current emitted by highly conducting Taylor cones. *Journal of Fluid Mechanics*, 260, 1994.

[37] M.Tajmar, C.Scharlemann, A.Genovese, N.Buldrini, W.Steiger, and I.Vasiljevich. Liquid-metal-ion source development for space propulsion at ARC. *Ultramicroscopy*, 109, 2009.

[38] R.R.Hofer, M.L.R.Walker, and A.D.Gallimore. A Comparison of Nude and Collimated Faraday Probes for Use with Hall Thrusters. In *27th International Electric Propulsion Conference*, 2001.

[39] M.Ye, Y.He, S.Hu, R.Wang, and T.Hu et al. Suppression of secondary electron yield by micro-porous array structure. *Journal of Applied Physics*, 113(074904), February 2013.

[40] C.Swanson and I.Kaganovich. Modeling of reduced secondary electron emission yield from a foam or fuzz surface. *Journal of Applied Physics*, 123(023302), January 2018.

[41] C.Huerta, M.I.Patino, and R.E.Wirz. Secondary electron emission from textured surfaces. *Journal Physics D:Applied Physics*, 151(145202), March 2018.

[42] A.Ottaviano, S.Banerjee, and Y.Raitses. A rapid technique for the determination of secondary electron emission yield from complex surfaces. *Journal of Applied Physics*, 126(223301), December 2019.

[43] E.Huerta and E.Wirz. Ion-induced electron emission reduction via complex surface trapping. *AIP advances*, 9(125009), December 2019.

[44] Exxentis. Exxentis Website Homepage.

[45] V.Hugonnaud and S.Mazouffre. Optimization of a Faraday cup collimator for electric propulsion device beam study: Case of a Hall thruster. *Journal of Vacuum Science and Technology A*, 2021.

[46] R.R.Hofer and A.D.Gallimore. High-Specific Impulse Hall Thrusters, Part 2: Efficiency Analysis. *Journal of Propulsion and Power*, 22(4).

[47] K.Dannenmayer and S.Mazouffre. Elementary scaling relations for Hall effect thrusters. page 236:245.

[48] R.R.Hoffer and R.S Jankovsky. A Hall thruster performance model incorporating the effects of a multiply-charged plasma. In AIAA, editor, *AIAA*, number AIAA-2001-3322, 2001.